УДК 531

Physical Nature of Strengthening Mechanisms During Extremely Long-Term Operation of Rails*

Yu.F. Ivanov[1], A.A. Yuriev[2], V.E. Kormyshev[3], X. Chen[4], V.B. Kosterev[3], V.E. Gromov[3]

[1]Institute of High-Current Electronics SB RAS (Tomsk, Russia)
[2]JSC "Evraz-West-Siberian Metallurgical Works" (Novokuznetsk, Russia)
[3]Siberian State Industrial University (Novokuznetsk, Russia)
[4]Wenzhou University (Wenzhou, China)

Физическая природа механизмов упрочнения при экстремально длительной эксплуатации рельсов

Ю.Ф. Иванов[1], А.А. Юрьев[2], В.Е. Кормышев[3], С. Чэнь[4], В.Б. Костерев[3], В.Е. Громов[3]

[1]Институт сильноточной электроники СО РАН (Томск, Россия)
[2]АО «Евраз-объединенный Западно-Сибирский металлургический комбинат» (Новокузнецк, Россия)
[3]Сибирский государственный индустриальный университет (Новокузнецк, Россия)
[4]Университет Вэньчжоу (Вэньчжоу, Китай)

The quantitative estimation of strengthening mechanisms of rails' surface layer is carried out on the basis of regularities and formation mechanisms of structure-phase states revealed by the methods of modern physical materials science. It is performed at different depths of the rail head along the central axis and fillet of differentially quenched 100-meter rails after the extremely long-term operation (gross passed tonnage of 1411 mln tons). A long-term operation of rails is accompanied by the formation of structural constituent gradient consisting of a regular change in the relative content of lamellar pearlite, fractured pearlite, the structure of ferrite-carbide mixture, scalar, and excess dislocation density along the cross-section of the rail head. As the distance to the rail fillet surface decreases, the relative content of metal volume with lamellar pearlite decreases. However, the relative content of metal volume with the presence of the fractured pearlite structure and ferrite-carbide mixture increases. The contributions caused by the matrix lattice friction, intraphase boundaries, dislocation substructure, presence of carbide particles, internal stress fields, solid-solution strengthening, pearlite component of steel structure are estimated. It is shown that the main mechanism of strengthening in the surface layer is due to the interaction of moving dislocations with low-angle boundaries of nanometer dimensional fragments and subgrains. The main dislocation strengthening mechanism in a near-surface layer at a depth of 2–10 mm is due to the interaction of moving dislocations with immobile ones.

Проведена количественная оценка механизмов упрочнения поверхностного слоя на основе закономерностей и механизмов формирования структурно-фазовых состояний, выявленных методами современного физического материаловедения на разной глубине головки рельса по центральной оси и выкружке дифференцированно закаленных 100-метровых рельсов после экстремально длительной эксплуатации (пропущенный тоннаж 1411 млн тонн). Длительная эксплуатация рельсов сопровождается формированием градиента структурных составляющих, заключающегося в закономерном изменении относительного содержания пластинчатого перлита, разрушенного перлита и скалярной структурой феррит-карбидной смеси и избыточной плотности дислокаций по сечению головки рельсов. По мере приближения к поверхности выкружки рельсов относительное содержание объема металла со структурой пластинчатого перлита снижается, а со структурой разрушенного перлита и феррито-карбидной смеси увеличивается. Оценены вклады трения решетки матрицы, внутрифазных границ, дислокационной субструктуры, наличия карбидных частиц, полей внутренних напряжений, твердорастворного упрочнения, перлитной составляющей структуры стали. Показано, что в поверхностном слое основной механизм упрочнения обусловлен взаимодействием движущихся дислокаций с малоугловыми границами

* Analysis of structure-phase state of steel is supported by RFBI grant (project № 19-32-60001), analysis of strengthening mechanisms is supported by of RSF grant (project № 19-19-00183).

Key words: strengthening mechanisms, structure, surface layers, rail head, long-term operation.

фрагментов и субзерен нанометрового размера. В приповерхностном слое на глубине 2–10 мм основной механизм упрочнения связан с взаимодействием движущихся дислокаций с неподвижными.

Ключевые слова: механизмы упрочнения, поверхностные слои, структура, головка рельса, длительная эксплуатация.

DOI: 10.14258/izvasu(2021)1-05

Introduction

Nowadays up to 85 % of freight and more than 50% of passenger transportations are carried by railway transport globally. A considerable increase in the intensity of railway transport and its freight traffic density has recently been observed. It requires a high operational resistance of rails. The differential quenching technology of 100-meter rails is used to solve these problems. The formation and evolution of structure-phase states and properties of rails' surface layers in long-term operation present a complex group of interrelated scientific and technical problems. The importance of the information is determined by the depth of understanding of condensed state physics fundamental problems, on the one hand, and the practical importance of the problem, on the other [1, 2].

It is apparent that there are different processes (recrystallization, relaxation processes, phase transitions, decay and formation of phases, amorphization, etc.) influenced by deformation during the long-term operation. The processes lead to the evolution of structural phase states and are accompanied by the formation of structural phase gradients [1–4]. Therefore, the revealing of nature and regularities of structure, phase composition, and defective substructure in a rail head at long operation is of utmost importance.

In recent years the problems related to the strengthening and wearing of rails have been surveyed in detail in the papers [3–9]. The formation of high operating properties of rails should be based on the knowledge of mechanisms of structural-phase changes and strengthening along the cross-section of rails in their long-term operation. It is possible to reveal the mechanisms only by analyzing the regularities of parameter evolution of fine structure and estimating the contributions of structural components and defect substructures to rails' strengthening in long-term operation.

For interim tests (passed tonnage of 691.8 mln tons gross weight), the data bank on the regularities of formation of structural phase states and a dislocation substructure, the distribution of carbon atoms in the head of long differentially quenched rails along the central axis and along fillet after the long-term operation has been developed in researches [10]. The gradient character of the structure, phase composition, and defect substructure being characterized by the regular change in scalar and excess dislocation density, the curvature-torsion of the crystal lattice and the degree of strain transformation of lamellar pearlite structure along the cross-section of a rail head have been studied.

The theoretical estimates of metallic additive yield point along the central axis and along the fillet are performed, in terms of physical material science, using the multi-aspect analysis of strengthening caused by carbide phase particles, by the formation of pearlite structure and dislocation substructure, by long-range stress fields and by solid-solution strengthening. The contributions into rail strengthening after passed tonnage of 500 and 1000 mln tons for bulk quenched 25-meter rails are assessed, and physical mechanisms are evaluated in research [11].

This study aims to quantitatively estimate the strengthening mechanisms of surface layers of differentially quenched 100-meter rails along the central axis and along fillet after extremely long-term operation.

Material and methods of investigation

The rails of the DT350 category with the gross passed tonnage of 1411 mln tons are taken from the Experimental ring track of the Russian Railways for further research. The certified batch of rails has been manufactured by OJSC 'Evraz-West Siberian Metallurgical Plant' in June 2013 following the requirements of the Technical Specifications 0921-276-01124323-2012 and undergone the differential thermal strengthening. The chemical composition of a rail metal sample meets the requirements of the Russian Standard P 51685-2013.

The examinations of a metal structure are carried out using the methods of optical microscopy (metallographic microvisor μVizo-MET-221P), scanning electron microscopy (MIRA3 Tesan), X-ray structural analysis (X-ray diffractometer XRD-7000S (Shimadzu, Japan)), and transmission electron diffraction microscopy (device EM-125) [12–14]. The samples (150–200 nm thick foils) examined by the transmission electron microscopy are manufactured by electrolytic thinning of plates cut out by electric spark erosion of metal and located near tread surfaces at a distance of 0, 2, and 10 mm. The diagram of sample preparation is shown in Fig. 1.

The hardness is measured at the tread surface according to the Brinell and Rockwell methods and following the Technical Specifications TU 0921-276-01124323-2012. In addition, the hardness is also measured at the upper part of the rail neck (≈30 mm higher than specified by state-

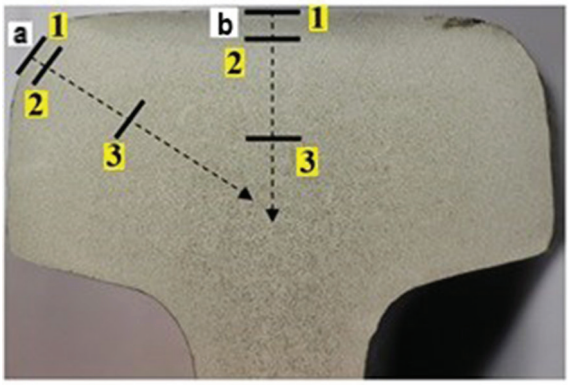

Fig. 1. Diagram of sample preparations for TEM studying. 1 tread surface, 2 layer at a distance of 2 mm from the surface, 3 layer at a distance of 10 mm from the surface. a) fillet; b) central axis

ment 6 of article 1.8.1 TU 0921-276-01124323-2012) and along the cross-section of the rail neck in the transverse direction at a distance of 2 mm, 10 mm, and 22 mm from the tread surface of a rail head along the vertical axis of symmetry. The microhardness is tested by the Vickers method with the indenter loading of 300 mN and a distance of 2 mm and 10 mm from the tread surface, with 5 measurements in each zone, using the PMT-3 equipment.

Results and Discussion

The complex quantitative studies of structure, phase composition, defect substructure, and tribological properties at a different distance from the tread surface along the central axis and along the fillet have been carried out in our works [15–19].

It is stated that the rail structure in the layer located at a distance of 10 mm from the surface is formed by pearlite grains of lamellar morphology. The regions of 'degenerate pearlite' and grains of structurally-free ferrite (ferrite grains in a volume of which cementite particles are absent) are present in negligible quantity.

The deformed pearlite can be found at a distance of 2.0 mm from the working surface in addition to the constituents mentioned above. It contains the cementite plates fractured into separate parts being displaced relative to each other (Fig. 2, a). The structure that we call the 'ferrite-carbide mixture' is also formed in the surface layer (Fig. 2, b).

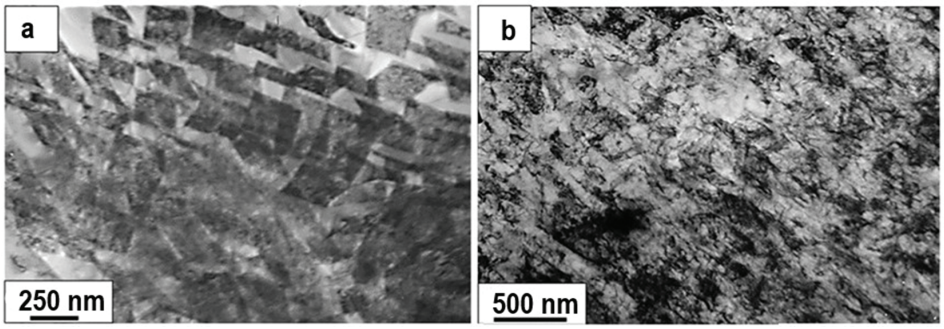

Fig. 2. Structure of rail metal; a — fractured lamellar pearlite; b — ferrite-carbide mixture; a — layer at the depth of 2 mm; b — surface layer of fillet

The characteristic feature of the structure is a nanodimensional range of grains, subgrains, and particles of the carbide phase forming it. The size of grains and subgrains forming the type of structure varies in the limits of 40-70 nm (Fig. 3, a). The size of carbide phase particles located along the boundaries of grains and subgrains varies in the limits of 8-20 nm (Fig. 3, b).

The relative content of structural constituents of rail metal shown in Figs. 2–3 varies according to Fig. 4 a.

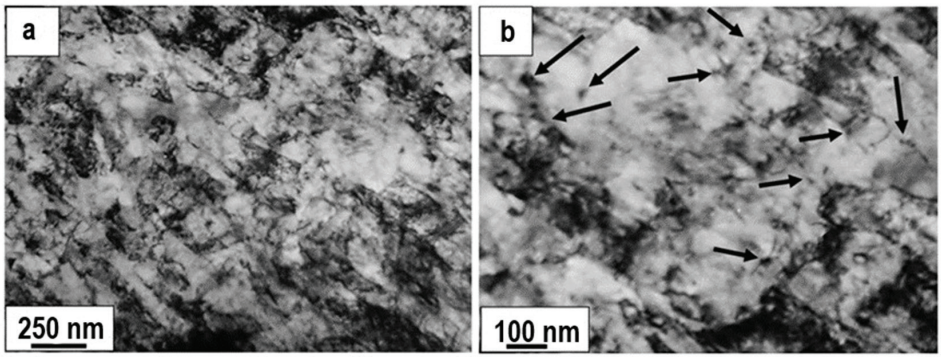

Fig. 3. Electron microscopic images of 'ferrite-carbide mixture' structure. Arrows indicate in (b) the particles of carbide phase

It is clearly seen that long-term rail operation is accompanied by the formation of structural constituents' gradient. It includes the regular decrease in the relative content of material volume with lamellar pearlite structure and the increase in that with the structure of fractured pearlite and ferrite-carbide mixture as the fillet surface is approached.

It is stated by the methods of transmission electron microscopy that the dislocation substructure is present in the ferrite constituent of pearlite colonies and the grains of structure-free ferrite. Following the classification given in [20, 21], the dislocations form tangles and networks or are distributed chaotically. The results presented in Fig. 4, b testify that the scalar dislocation density of rails increases as the fillet surface is approached. Scalar dislocation density increases the most intensively in lamellar pearlite structure, the least intensively — in degenerate pearlite and fractured pearlite structure.

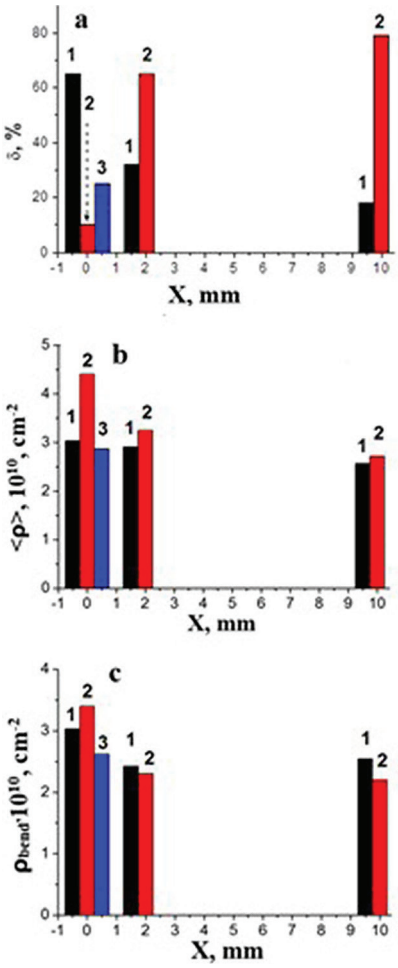

Fig. 4. Diagram of relative content of rail structural constituents (a), scalar (b) and excess (c) dislocation density gradient, X — distance from the working fillet surface; 1— degenerate perlite + fractured pearlite; 2 — lamellar pearlite; 3 — ferrite-carbide mixture

The long-term operation of rails is accompanied by the formation of internal stress fields in steel. The research conducted by transmission electron microscopy methods reveals the presence of stress fields in the material as the appearance of bend extinction contours [22] indicating the curvature-torsion of the crystal lattice of the foil part.

The estimation procedure of internal stress fields' value is reduced to the determination of curvature-torsion of crystal lattice χ [20–22]:

$$\chi = \frac{\partial \phi}{\partial \ell} = \frac{0.017}{h}$$

where h is transverse sizes of bend extinction contour.

The value of excess dislocation density ρ± is related to curvature-torsion gradient of the crystal lattice χ through absolute value of the Burgers dislocation vector b:

$$\rho_{\pm} = \frac{1}{b} \cdot \frac{\partial \phi}{\partial \ell}$$

Thus, having determined the transverse sizes of bend extinction contour of various structural constituents of steel experimentally, it is possible to estimate the value of excess dislocation density.

Analyzing the results in Fig. 4, c, it may be noted that excess dislocation density value reaches the largest magnitudes in lamellar pearlite structure, while the least onesin ferrite-carbide mixture structure. As the distance from the fillet surface increases, the value of excess dislocation density decreases, which testifies the decrease in the amplitude of internal stress fields of rail metal.

It is established that the scale of localization of internal stress fields of rail material depends, in a regular way, on the distance from the fillet surface. It is found that the internal stress fields in the steel layer at a depth of ≈10 mm are localized in the bulk of the pearlite colony; the sources of stress fields are the interfaces of colonies or pearlite grains. The extinction contours in the layer at a depth of ≈2 mm are localized in the bulk of several ferrite plates. Finally, the extinction contours in the layer that forms the fillet surface are localized mainly in the bulk of individual ferrite plates. It means that the deformation effect that occurs during the long-term operation of rails results in the formation of a gradient of localization volume of internal stress fields of rail metal and, consequently, a substantial increase in the number of stress concentration that, in its turn, will facilitate the increase in the level of embrittlement and rails' failure.

Measurements of hardness done along the head cross-section in the transverse direction demonstrate that the HRC hardness at a depth of 2 mm is 37.1, at a depth of 10 mm — 35.8, at 22 mm — 35.6. Microhardness at a depth of 2 mm amounts to 1481 MPa; microhardness at a depth of 10 mm is substantially lower and amounts to 1210 MPa [15–17].

It is obvious that the detected difference in microhardness values in metal thickness is due to structure-phase change in steel having a place in rail operation. The results of the analysis of steel structure and phase composition mentioned above testify to a multi-factor strengthening

of the material. The obtained quantitative characteristics of steel structure presented in [15–19] permit one to examine the physical nature of the increase in steel strengthening, estimate its strengthening mechanisms, and identify the dominating mechanisms determining the steel strength being characterized by microhardness in the research. It is evident that it is impossible to consider all morphological and phase diversity of steel structure while determining the material microhardness. In this relation, the quantitative estimate of steel strengthening mechanisms will be realized on the basis of quantitative characteristics averaged in material volume (concerning volume fraction and characteristics of different substructure types). The estimates of strengthening mechanisms value are performed using widely accepted expressions presented in [23–37].

The contributions caused by friction of matrix lattice $\Delta\sigma_0$ [38], pearlite component of steel structure $\Delta\sigma(P)$ [38, 39], dislocation substructure $\Delta\sigma(\rho)$ [39–42], internal stress fields $\Delta\sigma(h)$ [1, 43], carbide phase particles $\Delta\sigma(part.)$ [44, 45], intraphase boundaries $\Delta\sigma(L)$ [1, 38], solid solution strengthening $\Delta\sigma(sol.\ sol.)$ [38, 46–48] are analyzed.

Hence, having obtained the quantitative characteristics of steel structure, it is possible to perform the analysis of physical mechanisms responsible for the evolution of hardness in steel in the process of rail operation in a first approximation and to detect the physical mechanisms of hardness gradient formation in rail steel.

The total yield point of steel σ in a first approximation based on the additivity principle that supposes the independent action of each of material strengthening mechanisms may be presented as a linear sum of contributions of individual strengthening mechanisms [1, 38, 39, 46, 49]:

$$\sigma=\Delta\sigma_0+\Delta\sigma(L)+\Delta\sigma(\rho)+\Delta\sigma(h)+\Delta\sigma(part.)+\Delta\sigma(sol.\ sol.)+\Delta\sigma(P).$$

The estimates of steel strengthening mechanisms are carried out using the results of quantitative analysis of steel structure presented in [15–19]. The estimated results are listed in Table.

Table

Estimates of strengthening mechanisms of rail metal being formed at different distances along central axis and along fillet in head of 100-meter differentially quenched rails after extremely long-term operation

Average parameters in material	Tread surface			Working fillet		
	10 mm	2 mm	Surface	10 mm	2 mm	Surface
$\Delta\sigma(P)$, MPa	142.5	161.5	85.5	152	152	95
$\Delta\sigma(L)$, MPa	0	0	473.3	0	0	1455.6
$\Delta\sigma(\rho)$, MPa	152.8	181	181.4	164	206	190.4
$\Delta\sigma(h)$, MPa	131.3	149	255	148.6	149.6	230.4
$\Delta\sigma(part.)$, MPa	154.1	148.5	107	80,6	222.9	195
$\Delta\sigma(sol.\ sol.)$, MPa	11	11	11.7	11	11	11,7
$\sigma=\sum_{i=1}^{n}\sigma_i$, MPa	591.7	651	1114	556.2	741.5	2178.1

The following facts may be noted when analyzing the results listed in Table. Firstly, steel strength is a multi-factor value determined by the joint action of a number of physical mechanisms. Secondly, the strength of rail metal depends on the distance to the head surface independent of the analysis site (along the central axis or along the symmetry axis of the fillet), which is in agreement with the results obtained while estimating the steel microhardness. Thirdly, the rail metal strength increases while approaching the head surface. Fourthly, the main mechanism of rail metal strengthening in a subsurface layer (in the layer located at a depth of 2–10 mm) of the rail head is a dislocation one caused by the interaction of moving dislocations with immobile dislocations ('forest' dislocations). Fifthly, in the surface layer of the rail head, the main mechanism of metal strengthening involves the interaction of moving dislocations with low-angle boundaries of nanometer-dimensional fragments and subgrains.

Conclusion

The analysis of strengthening mechanisms of rail head metal along the symmetry axis of the fillet and along the central axis (tread surface) is carried out. It is shown that the strengthening has a multi-factor character in both cases and is determined by the superposition of a number of physical mechanisms.

It is shown that the increase of microhardness and hardness of rail steel subjected to long-term operation has a multi-factor character and is due to several factors. Firstly, the substructural strengthening is caused by the formation of nanodimensional fragments whose boundaries are stabilized by carbide phase particles. Secondly, the strengthening by nanodimensional particles

of carbide phase is located in the volume of fragments and on dislocations (dispersion strengthening). Thirdly, the strengthening is introduced by internal stress fields being formed due to deformation incompatibility of adjacent grains, crystallites of different phases, presence of microcracks.

It is determined that there are several most important physical mechanisms ensuring the high strength properties of rail head metal subjected to the extremely long-term operation. It is a dislocation mechanism caused by the interaction of moving dislocations with the immobile dislocations ('forest' dislocations) in the subsurface layer (the layer located at a depth of 2–10 mm) of rail head. For the case of the surface layer of the rail head, it is the mechanism that involves the interaction of moving dislocations with low-angle boundaries of nanometer-dimensional fragments and subgrains.

References

1. Gromov V.E., Peregudov O.A., Ivanov Yu.F., Konovalov S.V., Yuriev A.A. Evolution of structural-phase states of rail metal in long-term operation. Novosibirsk, 2017.

2. Gromov V.E., Ivanov Yu.F., Yuriev A.B., Morozov K.V. Microstructure of quenched rails. Cambridge, 2016.

3. Ivanisenko Yu., Fecht H.J. Microstructure modification in the surface layers of railway rails and wheels // Steel tech. 2008. Vol. 3. № 1.

4. Ivanisenko Yu., Maclaren I., Souvage X., Valiev R.Z., Fecht H.J. Shear-induced α→γ transformation in nanoscale Fe–C composite // Acta Mater. 2006. Vol. 54. № 6. URL: https://doi.org/10.1016/j.actamat.2005.11.034.

5. Seo J.-W., Jun H.-K., Kwon S.-J., Lee D.-H. Rolling contact fatigue and wear of two different rail steels under rolling–sliding contact // International Journal of Fatigue. 2016. Vol. 83. URL: https://doi.org/10.1016/j.ijfatigue2015.10.012.

6. Lewis R., Christoforou P., Wang W.J., Beagles A., Burstow M., Lewis S.R. Investigation of the influence of rail hardness on the wear of rail and wheel materials under dry conditions (ICRI wear mapping project) // Wear. 2019. Vol. 430–431. URL: https://doi.org/10.1016/j.wear.2019.05.030.

7. Skrypnyk R., Ekh M., Nielsen J.C.O., Pålsson B.A. Prediction of plastic deformation and wear in railway crossings — Comparing the performance of two rail steel grades // Wear. 2019. Vol. 428–429. URL: https://doi.org/10.1016/j.wear.2019.03.019.

8. Kim D., Quagliato L., Park D., Kim N. Lifetime prediction of linear slide rails based on surface abrasion and rolling contact fatigue-induced damage // Wear. 2019. Vol. 420–421. URL: https://doi.org/10.1016/j.wear.2018.10.015.

9. Huang Y.B., Shi L.B., Zhao X.J., Cai Z.B., Liu Q.Y., Wang W.J. On the formation and damage mechanism of rolling contact fatigue surface cracks of wheel/rail under the dry condition // Wear. 2018. Vol. 400–401. URL: https://doi.org/10.1016/j.wear.2017.12.020.

10. Ivanov Yu.F., Gromov V.E., Yuriev A.A., Glezer A.M., Popova N.A., Peregudov O.A., Konovalov S.V. Contribution of different mechanisms to differentially tampered rail strengthening during long operation // Deformation and failure of metals. 2018. № 4.

11. Gromov V.E., Ivanov Yu.F., Morozov K.V., Peregudov O.A., Popova N.A., Nikonenko E.L. Rail strengthening mechanisms in long-term operation // Problems of ferrous metallurgy and materials science. 2015. № 4.

12. Egerton F.R. Physical Principles of Electron Microscopy. Basel, 2016.

13. Kumar C.S.S.R. Transmission Electron Microscopy. Characterization of Nanomaterials. New York, 2014.

14. Carter C.B., Williams D.B. Transmission Electron Microscopy. Berlin, 2016.

15. Kormyshev V.E., Gromov V.E., Ivanov Yu.F., Glezer A.M., Yuriev A.A., Semin A.P., Sundeev R.V. Structural phase states and properties of rails after long-term operation // Materials Letters. 2020. Vol. 268. URL: https://doi.org/10.1016/j.matlet.2020.127499.

16. Kormyshev V.E., Ivanov Yu.F., Gromov V.E., Yuryev A.A., Polevoy E.V. Structure and properties of differentiatedly quenched 100-meter rails after extremely long operation // Fundamental problems of modern materials science. 2019. Vol. 16. № 4. DOI: 10.25712/ASTU.1811-1416.2019.04.016.

17. Kormyshev V.E., Polevoy E.V., Yuryev A.A., Gromov V.E., Ivanov Yu.F. Structure formation of differentiatedly quenched 100-meter rails in long-term operation // Izvestiya. Ferrous Metallurgy. 2020. Vol. 63. № 2. DOI: 10.17073/0368-0797-2020-2-108-115.

18. Kormyshev V.E., Ivanov Yu.F., Yuriev A.A., Polevoy E.V., Gromov V.E., Glezer A.M. Evolution of structural-phase states and properties of differentiatedly quenched 100-meter rails in extremely long-term operation. Information 1. Structure and properties of rail steel before operation // Problems of ferrous metallurgy and materials science. 2019. № 4.

19. Kormyshev V.E., Gromov V.E., Ivanov Yu.F., Glezer A.M. Structure of differentiatedly quenched rails under severe plastic // Deformation and failure of materials. 2020. № 8. DOI: 10.31044/1814-4632-2020-8-16-20.

20. Hirsch P., Hovy A., Nickolson R., Pashley D., Whelan M. Electron microscopy of fine crystals. M., 1968.

21. Koneva N.A., Kozlov E.V. Nature of substructural strengthening // Proceedings of Higher Schools. Physics. 1982. № 8.

22. Kozlov E.V., Starenchenko V.A., Koneva N.A. Evolution of dislocation substructure and thermodynamics of plastic deformation of metallic materials // Metals. 1993. Vol. 5.

23. Yao M.J., Welsch E., Ponge D., Haghighat S.M.H., Sandlöbes S., Choi P., et al. Strengthening and strain hardening mechanisms in a precipitation-hardened high-Mn lightweight steel // Acta Materia. 2017. Vol. 140. URL: https://doi.org/10.1016/j.actamat.2017.08.049.

24. Friedman L.H., Chrzan D.C. Scaling Theory of the Hall-Petch Relation for Multilayers // Phys. Rev. Lett. 1998. Vol. 81.

25. Han Y., Shi J., Xu L., Cao W.Q., Dong H. TiC precipitation induced effect on microstructure and mechanical properties in low carbon medium manganese steel // Mater. Sci. Eng. A. 2011. Vol. 530.

26. Zurob H.S., Hutchinson C.R., Brechet Y., Purdy G. Modeling recrystallization of microalloyed austenite: effect of coupling recovery, precipitation and recrystallization // Acta Mater. 2002. Vol. 50. URL: https://doi.org/10.1016/S1359-6454(02)00097-6.

27. Huthcinson B., Hagstrom J., Karlsson O., Lindell D., Tornberg M., Lindberg F., et al. Microstructures and hardness of as-quenched martensites (0.1–0.5%C) // Acta Mater. 2011. Vol. 59. URL: https://doi.org/10.1016/j.actamat.2011.05.061.

28. Kim J.G., Enikeev N.A., Seol J.B., Abramova M.M., Karavaeva M.V., Valiev R.Z., et al. Superior Strength and Multiple Strengthening Mechanisms in Nanocrystalline TWIP Steel // Scientific Reports. 2018. Vol. 8.

29. Sevillano J.G. An alternative model for the strain hardening of FCC alloys that twin, validated for twinning-induced plasticity steel // Scr. Mater. 2009. Vol. 60. URL: https://doi.org/10.1016/j.scriptamat.2008.10.035.

30. Bouaziz O., Allain S., Scott S. Effect of grain and twin boundaries on the hardening mechanisms of twinning-induced plasticity steels //Scr. Mater. 2008. Vol. 58. URL: https://doi.org/10.1016/j.scriptamat.2007.10.050.

31. Ganji R.S., Karthik P.S., Rao K.B.S., Rajulapati K.V. Strengthening mechanisms in equiatomic ultrafine grained AlCoCrCuFeNi high-entropy alloy studied by micro- and nanoindentation methods // Acta Mater. 2017. Vol. 125. URL: https://doi.org/10.1016/j.actamat.2016.11.046.

32. Silva R.A., Pinto A.L., Kuznetsov A., Bott I.S. Precipitation and Grain Size Effects on the Tensile Strain-Hardening Exponents of an API X80 Steel Pipe after High-Frequency Hot-Induction Bending // Metals. 2018. Vol. 8.

33. Hosford W.F. Mechanical Behavior of Materials, 2nd ed. Cambridge, 2010.

34. Morales E.V., Gallego J., Kestenbachz H.-J. On coherent carbonitride precipitation in commercial microalloyed steels // Philos. Mag. Lett. 2003. Vol. 83.

35. Morales E.V., Galeano Alvarez N.J., Morales A.M., Bott I.S. Precipitation kinetics and their effects on age hardening in an Fe–Mn–Si–Ti martensitic alloy // Mater. Sci. Eng. A. 2012. Vol. 534. URL: https://doi.org/10.1016/j.msea.2011.11.056.

36. Sieurin H., Zander J., Sandström R. Modelling solid solution hardening in stainless steels // Mater. Sci. Eng. A. 2006. Vol. 415. URL: https://doi.org/10.1016/j.msea.2005.09.031.

37. Fine M.E., Isheim D. Origin of copper precipitation strengthening in steel revisited // ScriptaMaterialia. 2005. Vol. 53. URL: https://doi.org/10.1016/j.scriptamat.2005.02.034.

38. Goldstein M.I., Farber B.M. Dispersion hardening of steel. M., 1979.

39. Pickering F.B. Physical metal science and treatment of steels. M., 1982.

40. Predvoditelev A.A. Modern state of investigation into dislocation ensembles. In book: Problems of modern crystallography. M., 1975.

41. Mc. Li D. Mechanical properties of metals. M., 1965.

42. Embyri I.D. Strengthening Method in Crystals. Applied Science Publishes, 1971.

43. Koneva N.A., Kozlov E.V. Structural levels of plastic deformation and failure. Novosibirsk, 1990. Chapter. Physical nature of stage development of plastic deformation.

44. Schtremel M.A. Strength of alloys. Part II. Deformation. Text-book for Higher Schools. M., 1997.

45. Mott N.F., Nabarro F.R.N. The distribution of dislocations in slip band // Proc. Phys. Soc. 1940. Vol. 52. № 1.

46. Belen'kiy B.Z., Farber B.M., Goldschtein M.I. Estimations of strength of low-carbon low-alloy steels according to structural data // Physics of metals and material science. 1975. Vol. 39. № 3.

47. Ridley T., Stuart H., Zwell L. Lattice parameters of Fe-C austenite of room temperature // Trans. Met. Soc. AIME. 1969. Vol. 246. № 8.

48. Vohringer O., Macherauch E. Structure and Mechanischeeigenchaft von martensite // H.T.M. 1977. Vol. 32. № 4.

49. Prnka T. Quantitative relations between parameters of dispersed precipitations and mechanical properties of steels // Metal science and thermal treatment of steel. 1979. № 7.